

# Determining Kitaev interaction in spin- $S$ honeycomb Mott insulators

Jiefu Cen<sup>1</sup> and Hae-Young Kee<sup>1,2,\*</sup>

<sup>1</sup>*Department of Physics, University of Toronto, Toronto, Ontario, Canada M5S 1A7*

<sup>2</sup>*Canadian Institute for Advanced Research, CIFAR Program in Quantum Materials, Toronto, Ontario, Canada, M5G 1M1*

The Kitaev interaction in a honeycomb lattice with higher-spin  $S$  has been one of the central attractions, as it may offer quantum spin liquids. A microscopic theory showed that when the Hund's coupling at the transition metal generates  $S > \frac{1}{2}$ , the spin-orbit coupling at the heavy ligands provides a route to the Kitaev interaction. However, there have been debates over its strength compared to other symmetry-allowed interactions. Investigating the symmetry of the Hamiltonian for general  $S$ , we show the magnon energies at two momentum points related by a broken mirror symmetry reflect the Kitaev interaction when a magnetic field is in the mirror plane. Applying the symmetry analysis to  $\text{CrI}_3$  with  $S = \frac{3}{2}$  together with the available angle-dependent ferromagnetic resonance data, we estimate the Kitaev interaction out of the full Hamiltonian and find that it is sub-dominant. Our theory can be tested by inelastic neutron scattering on candidate materials under the proposed magnetic field direction, which will advance the search for general  $S$  Kitaev materials.

*Introduction* – The Kitaev interaction in a honeycomb lattice has attracted much attention as it offers the exactly solvable Kitaev quantum spin liquid for spin  $S = \frac{1}{2}$  [1–13]. The higher-spin Kitaev model has been theoretically studied [14–16], and numerical results have suggested that its ground state exhibits a quantum spin liquid [17–21]. Recently, a microscopic theory to realize higher  $S$  in two-dimensional (2D) materials was proposed. The bond-dependent Kitaev and symmetric off-diagonal interactions denoted by  $\Gamma$  and  $\Gamma'$  were derived using the strong coupling approach [22]. These interactions originate from the strong spin-orbit coupling (SOC) at the heavy ligands together with the Hund's coupling at transition metal sites. Shortly after, it was suggested that  $\text{CrI}_3$  with ferromagnetic (FM) ordering at low temperature is a Kitaev candidate material with  $S = \frac{3}{2}$  where the Kitaev interaction is dominant over other symmetry-allowed interactions [23]. However, its strength compared to other interactions such as the most conventional Heisenberg term has been much debated [24, 25].

Here we study the extended Kitaev model containing all the symmetry-allowed interactions with spin  $S$  in a honeycomb lattice to address the significance of the Kitaev interaction. Based on the symmetry analysis in momentum space, we show that the magnon energies at two momenta related by a broken mirror symmetry reflect the presence of the bond-dependent interactions including the Kitaev, when a magnetic field is applied in the broken mirror plane. Applying the theory to  $\text{CrI}_3$  together with the currently available angle-dependent ferromagnetic resonance (FMR) data, we find the Kitaev interaction to be sub-dominant, i.e., the second largest after the Heisenberg interaction. Our proposal can be tested by inelastic neutron scattering (INS) under the magnetic field in the broken mirror plane. The suggested experimental setup can be extended to general models for any  $S$ .

*Spin Model for general spin  $S$*  – Let us begin with the

general Hamiltonian and inspect its symmetry. The spin exchange Hamiltonian for spin  $S$  on the ideal honeycomb lattice is known as the  $JK\Gamma$  model [3], where  $J$ ,  $K$  and  $\Gamma$  are Heisenberg, Kitaev and symmetric off-diagonal interactions respectively. When trigonal distortion is introduced, the single-ion anisotropy and another off-diagonal interaction denoted by  $\Gamma'$  are also present [26]. Transforming the octahedral  $xyz$  axes to the crystallographic  $abc$  axes shown in Fig. 1(a), the general Hamiltonian beyond nearest neighbor (n.n.) is given by [27–30]

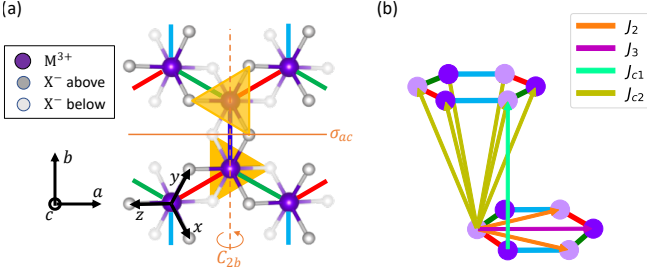
$$\begin{aligned} \mathcal{H} = \sum_{\langle i,j \rangle} & \left[ J_{XY}(S_i^a S_j^a + S_i^b S_j^b) + J_Z S_i^c S_j^c \right. \\ & + J_{ab} [c_{\phi_\gamma}(S_i^a S_j^a - S_i^b S_j^b) - s_{\phi_\gamma}(S_i^a S_j^b + S_i^b S_j^a)] \\ & \left. - \sqrt{2} J_{ac} [c_{\phi_\gamma}(S_i^a S_j^c + S_i^c S_j^a) + s_{\phi_\gamma}(S_i^b S_j^c + S_i^c S_j^b)] \right] \\ & + \sum_i A_c (S_i^c)^2 + \sum_{\langle\langle i,j \rangle\rangle} D_c \text{sgn}(ij) (S_i^a S_j^b - S_i^b S_j^a) \\ & + \sum_{(i,j)_n} J_n \mathbf{S}_i \cdot \mathbf{S}_j, \end{aligned} \quad (1)$$

where  $c_{\phi_\gamma} = \cos \phi_\gamma$ ,  $s_{\phi_\gamma} = \sin \phi_\gamma$  and  $\phi_\gamma = 0, \frac{2\pi}{3}$  and  $\frac{4\pi}{3}$  for  $\gamma = z, x$ - and  $y$ -bond respectively.  $A_c$  and  $D_c$  are single-ion anisotropy due to the trigonal distortion and the second n.n. Dzyaloshinskii-Moriya (DM) interaction with the D-vector along the  $c$ -axis [25], respectively.  $J_n$  are Heisenberg interactions between further neighbors and interlayers denoted by  $(i,j)_n$ , as shown in Fig. 1(b). They are much smaller than the n.n. interactions.

The bond-dependent exchange interactions,  $J_{ab}$  and  $J_{ac}$  with  $\phi_\gamma$  are related to  $J$ ,  $K$ ,  $\Gamma$  and  $\Gamma'$  as follows:

$$\begin{aligned} J_{XY} &= J + J_{ac} - \Gamma', \quad J_Z = J + J_{ab} + 2\Gamma', \\ J_{ab} &= \frac{1}{3}K + \frac{2}{3}(\Gamma - \Gamma'), \quad J_{ac} = \frac{1}{3}K - \frac{1}{3}(\Gamma - \Gamma'). \end{aligned} \quad (2)$$

A combination of  $\Gamma$  and  $\Gamma'$  leads to the in- and out-of-plane magnetic anisotropy and the spin gap at zero



momentum since  $J_Z - J_{XY} = \Gamma + 2\Gamma'$ . The single-ion anisotropy  $A_c$  also generates the anisotropy and spin gap except  $S = \frac{1}{2}$ , for which it is a constant. Below we will first analyze the symmetry of the Hamiltonian.

**Symmetry Analysis** – The symmetries of the Hamiltonian were analyzed for  $S = \frac{1}{2}$  in Ref. [30]. For general  $S$  including combined symmetry operations, they are summarized in the first row of Table I. The cross and circle refer to broken and preserved symmetries, respectively.  $\mathcal{T}$  is the time reversal symmetry  $\mathcal{T} : \mathbf{S} \rightarrow -\mathbf{S}$ .  $C_{3c}$  is the  $\frac{2\pi}{3}$  rotation of the lattice around the  $\hat{c}$  axis.  $C_{2a}$  and  $C_{2b}$  are  $\pi$  rotations about the  $\hat{a}$  and  $\hat{b}$  axes respectively. The spatial inversion and translation symmetries are intact. Since the octahedron forms two triangles above and below the transition metal  $M$  plane as shown in Fig. 1 (a), the mirror plane exists only in the  $ac$  plane equivalent to  $C_{2b}$  because of spatial inversion. The mirror symmetry about the  $bc$  plane (i.e.,  $C_{2a}$ ) is broken, which results in a finite  $J_{ac}$  in the Hamiltonian. The red crosses are the broken symmetries due to a finite  $J_{ac}$ , and the blue circles are the preserved symmetries if  $J_{ac}$  was zero.

The second and third rows show how the symmetries are affected under special magnetic field directions. When the magnetic field is applied,  $\mathcal{T}$  is broken.  $C_{3c}$  is also broken as the field is away from the  $c$ -axis. The combined operation  $\mathcal{T}C_{2b}$  is preserved when the field is in the  $ac$  plane, while it is broken when the field is in the  $bc$  plane. It is important to note that another combined operation  $\mathcal{T}C_{2a}$  is preserved if  $J_{ac}$  was absent, as indicated by the blue circle. Since the lack of  $\mathcal{T}C_{2a}$  is only related to a finite  $J_{ac}$  in  $\mathcal{H}$  while all the other symmetries are broken by the field, the difference in the spin excitations between two momenta related by  $\mathcal{T}C_{2a}$  is only due to  $J_{ac}$ , i.e., the magnon energy difference between these two momenta can be used to determine  $J_{ac}$ .

**A Simple Example** – Based on the symmetry relation summarized in table I, we investigate the spin wave under a magnetic field in the  $bc$  plane. We expect that the dif-

	$C_{3c}$	$C_{2b}$	$\mathcal{T}C_{2b}$	$C_{2a}$	$\mathcal{T}C_{2a}$
$\mathbf{h} = 0$	○	○	○	×/○	×/○
$\mathbf{h}$ in $ac$ plane	×	×	○	×	×
$\mathbf{h}$ in $bc$ plane	×	×	×	×	×/○

TABLE I. Symmetries of the Hamiltonian under the magnetic field in specific planes. The cross and circle refer to broken and preserved symmetries respectively. The red cross indicates the broken symmetry due to a finite  $J_{ac}$ , and the blue circle the preserved symmetry if  $J_{ac}$  was absent. We assume that the spatial inversion and translation symmetries are intact, and there is no spontaneous symmetry breaking due to magnetic ordering.

ference in magnon energy between two momenta related by  $\mathcal{T}C_{2a}$  will signal the presence of  $J_{ac}$ .

As an example, we check the simple case of  $J = -1$ ,  $K = 0.5$ , and set  $g\mu_B h = 1$ . The spin wave with the field in the  $bc$  plane with an angle of  $\theta = 45^\circ$  is shown in Fig. 2(a)-(b). The momentum paths  $\Gamma - M_1 - K_1$  and  $\Gamma - M_3 - K_2$  shown Fig. 2(c) are related by the combination  $\mathcal{T}C_{2a}$ . The excitations along these two paths are different since  $C_{2a}$  reflects the nonzero Kitaev interaction due to the broken  $bc$ -plane mirror symmetry. For example, the white arrows indicate the significant difference in the energies between  $M_1$  and  $M_3$  (see the Supplemental Material for detailed analysis). However, the paths  $K_1 - M_2$  and  $K_2 - M_2$  have the same energies because the spatial inversion symmetry ( $\mathbf{k} \rightarrow -\mathbf{k}$ ) is still intact.

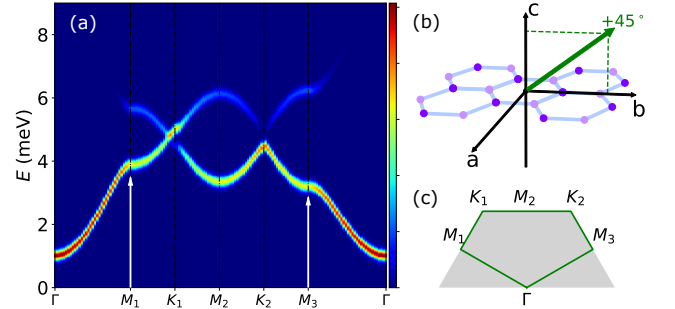


FIG. 2. Magnon spectrum with  $J = -1$  and  $K = 0.5$  under a magnetic field in the  $b - c$  plane with an angle of  $\theta = 45^\circ$  and the strength of  $g\mu_B h = 1$ . The difference between  $M_1$  and  $M_3$  highlighted by the white arrows is due to the Kitaev interaction.

While the current analysis of measuring the finite  $J_{ac}$  works for any spin  $S$ , estimating the Kitaev interaction out of  $J_{ac}$ , which is a combination of  $K$ ,  $\Gamma$  and  $\Gamma'$ , depends on the size of  $S$ . For  $S > 1/2$ , it was shown that  $\Gamma = 0$  up to the 4th order perturbation in  $d^8$  systems like  $\text{Ni}_2$  with  $S=1$ [22], and  $\Gamma, \Gamma' \ll A_c$  and  $\Gamma \sim \Gamma'$  resulting in  $J_{ac} \sim K/3$  for  $\text{CrI}_3$  with  $S = \frac{3}{2}$  [31]. On the other hand, for  $S = \frac{1}{2}$ ,  $\Gamma$  is significant while  $\Gamma'$  can be ignored when trigonal distortion is minimal [26]. Thus one has to subtract the  $\Gamma$  contribution from  $J_{ac}$  to determine

the Kitaev interaction. Since the in- and out-of-plane anisotropy mainly originates from  $\Gamma$  when there is no  $A_c$  for  $S = \frac{1}{2}$ , one can first determine  $\Gamma$  from the anisotropy and subtract  $\Gamma$  from  $J_{ac}$  to finalize the Kitaev. For  $\alpha$ - $\text{RuCl}_3$  [13, 32–34], a large effect of  $J_{ac}$  is expected in the magnon energy difference between  $M_1$  and  $M_3$ , as the Kitaev and  $\Gamma$  have opposite signs making  $J_{ac}$  large.

*Application to  $\text{CrI}_3$*  –  $\text{CrI}_3$  is a well-known quasi-2D van der Waals ferromagnet with the spin- $\frac{3}{2}$   $\text{Cr}^{3+}$  ions sitting on honeycombs of edge sharing octahedra. The FM order in bulk  $\text{CrI}_3$  persists to single-layer with a reduced transition temperature  $T_C \sim 45\text{K}$  [35], and there has been a lot of attention on the minimal 2D spin model. In particular, the strength of the Kitaev interaction in  $\text{CrI}_3$  has been debated. Based on the angle-dependent FMR data [23], Lee et al proposed that the Kitaev interaction is 25 times larger than the Heisenberg interaction ( $|K| \sim 25|J|$ ), and a tiny  $\Gamma$  interaction is necessary to have a finite spin gap at the ordering wavevector. The FMR data were fitted with calculations using the Smit-Beljers-Suhl equation with the free energy obtained from the partition function of a mean-field Hamiltonian.  $J$  and  $K$  were resolved by the additional fit to the  $T_C = 61\text{K}$  of the FM phase obtained by linear spin wave theory (LSWT). The large Kitaev interaction was also claimed to be responsible for the spin gap at the Dirac point.

On the other hand, Chen et al studied the magnon spectrum via the INS experiment under an in-plane magnetic field that aligns the spin moments in-plane [25]. In the FM ordered state, a well-defined magnon appeared. The earlier proposal with the dominant Kitaev interaction was ruled out because it did not fit the magnon spectrum under the in-plane field. Instead, they found that the FM Heisenberg interaction is dominant, and the significant DM interaction ( $D_c$ ) with an out-of-plane D-vector defined on the second n.n. bond opens up the spin gap at the Dirac point.

However, the measured INS data alone does not strongly constrain the strength of  $K$ , because the contribution of  $K$  to the spin gap is small compared to  $D_c$  due to the sizable difference in the pre-factors in LSWT. This calls for further investigation to determine  $K$ . As discussed above, for  $S > \frac{1}{2}$ ,  $\Gamma$  and  $\Gamma'$  are negligible, and  $J_{ac} \sim K/3$ . Since it is the Kitaev interaction that reflects the broken  $bc$  mirror symmetry, we can apply the symmetry analysis to estimate the Kitaev interaction in  $\text{CrI}_3$ . However, there is no experiment on  $\text{CrI}_3$  under the  $bc$ -plane field, so we will first determine the spin interactions using the available angle-dependent FMR and INS experiments. Then, we will present the magnon spectrum reflecting the Kitaev interaction under the  $bc$ -plane field, which can be tested in future experiments.

We first obtain the relative strength of the Kitaev interaction from the resonant magnetic field data in the FMR experiment by Lee et al. [23], where the magnetic field is applied in the  $ac$  plane as shown in the inset of

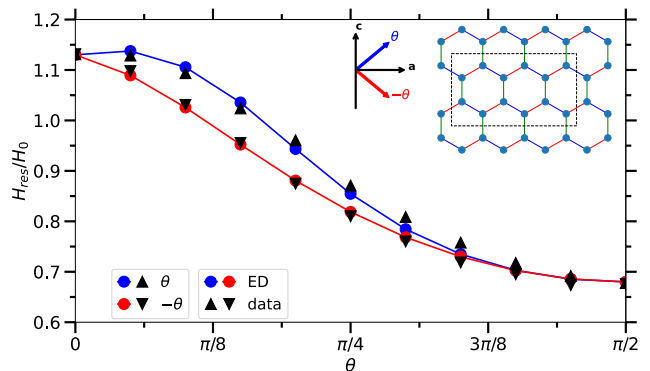


FIG. 3. FMR resonant field  $H_{\text{res}}$  at 240 GHz resonant frequency as the field angle  $\theta$  is varied, reproduce from Ref. [23].  $H_{\text{res}}$  is normalized by that of a free spin. The magnetic field angles are  $\pm\theta$  in the  $ac$  plane. Inset is the 12-site cluster used in the exact diagonalization (ED) of spin- $\frac{3}{2}$  to calculate the resonant field of our model. The calculation agrees with the FMR data well.

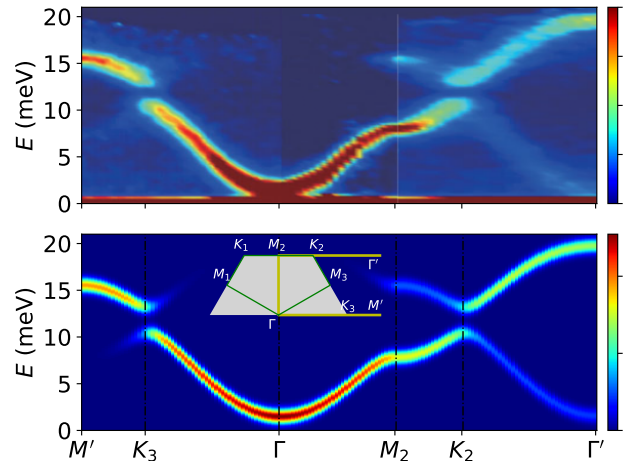


FIG. 4. (a) Inelastic neutron scattering (INS) data reproduced from Ref. [25] and (b) Magnon spectrum of our model without a magnetic field using linear spin wave theory (LSWT). The momentum path (yellow) is shown in the inset. The calculation agrees with the INS data well.

Fig. 3. Thus we use the symmetry of the  $ac$  plane proposed in Ref. [30]. The field direction is in the  $ac$  plane with angles  $\theta$  ( $0 < \theta < \pi/2$ ) above and below the honeycomb plane. The data for  $\theta$  and  $-\theta$  are shown by up- and down-triangles respectively in Fig. 3. Previous analysis of the FMR data using the free energy of a mean-field Hamiltonian could not account for bond-dependent interactions properly for spin excitations at zero momentum, so we use exact diagonalization (ED) [36]. The resonant field at each field angle is calculated by matching the 240 GHz resonant frequency to the zero-momentum spin excitation in the ED of a 12-site cluster shown in the inset of Fig. 3. The zero-momentum spin excitations have neg-

ligible finite-size effects with this magnetic field strength (see the Supplemental Material). In order to account for the difference in the resonant fields between  $\theta$  and  $-\theta$  as presented in Ref. [30], the relative strength between the Kitaev and Heisenberg interactions is required to be  $|K| \sim 0.4|J|$ . The single-ion anisotropy  $A_c$  and g-factor anisotropy  $g_{\perp} = 2.24$ ,  $g_{\parallel} = 1.69$  are determined from the in- and out-of-plane magnetic anisotropy of the resonant field. The calculated resonant field for our model is shown in Fig. 2 by blue ( $\theta$ ) and red ( $-\theta$ ) filled circles.

The Heisenberg  $J$  and Kitaev  $K$  interactions are then estimated using the INS data with no magnetic field by Chen et al. [25]. We use LSWT since the spin excitations are well defined due to the dominant FM Heisenberg  $J$ . The same small DM interaction ( $D_c$ ) with an out-of-plane D-vector and interlayer Heisenberg couplings ( $J_{c1}$ ,  $J_{c2}$ ) as suggested by Chen et al. [25] are used to account for the spin gap at the Dirac point and the out-of-plane momentum dependence respectively. Small second and third n.n. Heisenberg interactions ( $J_2$ ,  $J_3$ ) are added to improve the fit, but they do not alter the main findings. The INS data adopted from Ref. [25] is shown in Fig. 4(a) to make a comparison to the calculated spin wave spectrum without a field in Fig. 4(b). The interlayer couplings are taken into account by integrating over the out-of-plane momentum. All the small Heisenberg interactions have negligible effects on the FMR resonant field calculation shown in Fig. 3.

Interaction	value (meV)	Interaction	value (meV)
$J$	-2.5	$J_2$	-0.09
$K$	1.1	$J_3$	0.13
$\Gamma$	$\sim 0$	$J_{c1}$	0.048
$\Gamma'$	$\sim 0$	$J_{c2}$	-0.071
$A_c$	-0.23	$D_c$	0.17

TABLE II. Spin exchange interactions that can accommodate both the FMR and INS experiments for CrI<sub>3</sub>.

Table II lists the spin interactions obtained from the above analysis of the FMR and INS data. Note the samples used in the INS and FMR experiments are different, but we expect them to have similar intralayer couplings since the Cr-Cr distances are similar. The interlayer couplings can vary a lot due to the different  $c$ -axis layer spacing, but they do not affect the broken  $C_{2a}$  symmetry. Thus our method to determine the Kitaev interaction applies to both samples. Here we assume the samples to be perfect single crystals. However, the mosaicity of the sample in the FMR experiment is unknown, and the effect of sample mosaicity will be discussed later.

Using the obtained parameters of the spin model, we predict that the magnon spectrum under a  $bc$ -plane magnetic field should reflect the size of the Kitaev interaction. The result with a field angle of  $\theta = 45^\circ$  and a field strength of 8.6T is shown in Fig. 5. As expected, there is a noticeable difference in the magnon energies between

$M_1$  and  $M_3$ . In the Supplemental Material, we also show the magnon spectrum under two  $ac$ -plane fields for the obtained CrI<sub>3</sub> model.

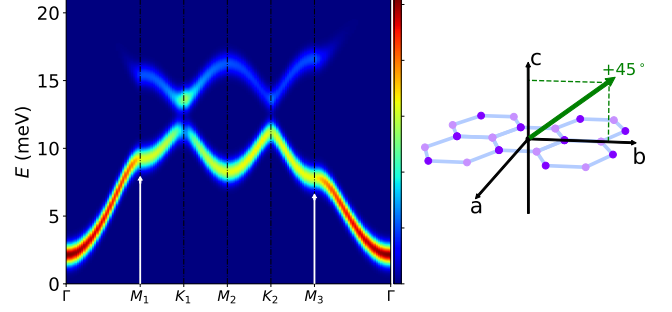


FIG. 5. Magnon spectrum of our model under a magnetic field in the  $bc$  plane with an angle of  $\theta = 45^\circ$  and a field strength of 8.6T. The difference between  $M_1$  and  $M_3$  highlighted by the white arrows is due to the Kitaev interaction.

*Summary and Discussion* – In summary, we show how to determine the Kitaev interaction for a general- $S$  model using the magnon energies at two momenta only related by the broken  $bc$ -plane mirror symmetry under the  $bc$ -plane field. We apply this method to CrI<sub>3</sub> with  $S = \frac{3}{2}$  and show that it is a sub-Kitaev material, i.e., the Kitaev interaction is the second largest after the FM Heisenberg interaction. We predict its magnon spectrum that reflects the strength of the Kitaev interaction. Our method here requires INS measurement for a fixed magnetic field, which is advantageous over the method described in Ref. [30] that needs INS measurements under rotated  $ac$ -plane fields, though it applies to zero-momentum excitations detected by optical spectroscopies such as angle-dependant FMR.

The relative strength of the Kitaev interaction for CrI<sub>3</sub> determined from the FMR data does not consider sample mosaicity. The effect of in-plane mosaicity can be estimated by applying a Gaussian filter in the in-plane field angle. The differences in the FMR resonances with the field angles above and below the honeycomb plane, which manifest the Kitaev interaction, are maximal when the field is in the  $ac$  plane. Thus, Gaussian averaging the in-plane field angle will always decrease the resonance energy differences. The strength of the Kitaev interaction in CrI<sub>3</sub> could be larger if the FMR sample had in-plane mosaicity, which needs to be clarified in the future.

This work was supported by the Natural Sciences and Engineering Research Council of Canada and the Canada Research Chairs Program. HYK thanks Aspen Center for Physics supported by National Science Foundation grant PHY-1607611, where a part of work was performed. This research was enabled in part by support provided by Sharcnet ([www.sharcnet.ca](http://www.sharcnet.ca)) and Compute Canada ([www.computecanada.ca](http://www.computecanada.ca)). Computations were performed on the GPC and Niagara supercomputers at

the SciNet HPC Consortium. SciNet is funded by: the Canada Foundation for Innovation under the auspices of Compute Canada; the Government of Ontario; Ontario Research Fund - Research Excellence; and the University of Toronto.

---

\* [hykee@physics.utoronto.ca](mailto:hykee@physics.utoronto.ca)

- [1] Alexei Kitaev, “Anyons in an exactly solved model and beyond,” *Ann. Phys. (N. Y.)* **321**, 2 – 111 (2006), January Special Issue.
- [2] G. Jackeli and G. Khaliullin, “Mott Insulators in the Strong Spin-Orbit Coupling Limit: From Heisenberg to a Quantum Compass and Kitaev Models,” *Phys. Rev. Lett.* **102**, 017205 (2009).
- [3] Jeffrey G. Rau, Eric Kin-Ho Lee, and Hae-Young Kee, “Generic spin model for the honeycomb iridates beyond the Kitaev limit,” *Phys. Rev. Lett.* **112**, 077204 (2014).
- [4] Yogesh Singh, S. Manni, J. Reuther, T. Berlijn, R. Thomale, W. Ku, S. Trebst, and P. Gegenwart, “Relevance of the Heisenberg-Kitaev model for the honeycomb lattice iridates  $A_2\text{IrO}_3$ ,” *Phys. Rev. Lett.* **108**, 127203 (2012).
- [5] S. K. Choi, R. Coldea, A. N. Kolmogorov, T. Lancaster, I. I. Mazin, S. J. Blundell, P. G. Radaelli, Yogesh Singh, P. Gegenwart, K. R. Choi, S.-W. Cheong, P. J. Baker, C. Stock, and J. Taylor, “Spin waves and revised crystal structure of honeycomb iridate  $\text{Na}_2\text{IrO}_3$ ,” *Phys. Rev. Lett.* **108**, 127204 (2012).
- [6] K. W. Plumb, J. P. Clancy, L. J. Sandilands, V. Vijay Shankar, Y. F. Hu, K. S. Burch, Hae-Young Kee, and Young-June Kim, “ $\alpha\text{-RuCl}_3$ : A spin-orbit assisted mott insulator on a honeycomb lattice,” *Phys. Rev. B* **90**, 041112(R) (2014).
- [7] K. A. Modic, Tess E. Smidt, Itamar Kimchi, Nicholas P. Breznay, Alun Biffin, Sungkyun Choi, Roger D. Johnson, Radu Coldea, Pilanda Watkins-Curry, Gregory T. McCandless, Julia Y. Chan, Felipe Gandara, Z. Islam, Ashvin Vishwanath, Arkady Shekhter, Ross D. McDonald, and James G. Analytis, “Realization of a three-dimensional spin-anisotropic harmonic honeycomb iridate,” *Nat. Commun.* **5**, 4203 (2014).
- [8] Heung-Sik Kim, Vijay Shankar V., Andrei Catuneanu, and Hae-Young Kee, “Kitaev magnetism in honeycomb  $\alpha\text{-RuCl}_3$  with intermediate spin-orbit coupling,” *Phys. Rev. B* **91**, 241110(R) (2015).
- [9] J. A. Sears, M. Songvilay, K. W. Plumb, J. P. Clancy, Y. Qiu, Y. Zhao, D. Parshall, and Young-June Kim, “Magnetic order in  $\alpha\text{-RuCl}_3$ : A honeycomb-lattice quantum magnet with strong spin-orbit coupling,” *Phys. Rev. B* **91**, 144420 (2015).
- [10] Luke J. Sandilands, Yao Tian, Kemp W. Plumb, Young-June Kim, and Kenneth S. Burch, “Scattering continuum and possible fractionalized excitations in  $\alpha\text{-RuCl}_3$ ,” *Phys. Rev. Lett.* **114**, 147201 (2015).
- [11] R. D. Johnson, S. C. Williams, A. A. Haghighirad, J. Singleton, V. Zapf, P. Manuel, I. I. Mazin, Y. Li, H. O. Jeschke, R. Valentí, and R. Coldea, “Monoclinic crystal structure of  $\alpha\text{-RuCl}_3$  and the zigzag antiferromagnetic ground state,” *Phys. Rev. B* **92**, 235119 (2015).
- [12] A. Banerjee, C. A. Bridges, J.-Q. Yan, A. A. Aczel, L. Li, M. B. Stone, G. E. Granroth, M. D. Lumsden, Y. Yiu, J. Knolle, S. Bhattacharjee, D. L. Kovrizhin, R. Moessner, D. A. Tennant, D. G. Mandrus, and S. E. Nagler, “Proximate Kitaev quantum spin liquid behaviour in a honeycomb magnet,” *Nature Materials* **15**, 733 (2016), article.
- [13] Heung-Sik Kim and Hae-Young Kee, “Crystal structure and magnetism in  $\alpha\text{-RuCl}_3$ : An ab initio study,” *Phys. Rev. B* **93**, 155143 (2016).
- [14] G. Baskaran, Saptarshi Mandal, and R. Shankar, “Exact results for spin dynamics and fractionalization in the kitaev model,” *Phys. Rev. Lett.* **98**, 247201 (2007).
- [15] G. Baskaran, Diptiman Sen, and R. Shankar, “Spin- $s$  kitaev model: Classical ground states, order from disorder, and exact correlation functions,” *Phys. Rev. B* **78**, 115116 (2008).
- [16] J. Oitmaa, A. Koga, and R. R. P. Singh, “Incipient and well-developed entropy plateaus in spin- $s$  kitaev models,” *Phys. Rev. B* **98**, 214404 (2018).
- [17] Akihisa Koga, Hiroyuki Tomishige, and Joji Nasu, “Ground-state and thermodynamic properties of an  $s = 1$  kitaev model,” *Journal of the Physical Society of Japan* **87**, 063703 (2018), <https://doi.org/10.7566/JPSJ.87.063703>.
- [18] Zheng Zhu, Zheng-Yu Weng, and D. N. Sheng, “Magnetic field induced spin liquids in  $s = 1$  kitaev honeycomb model,” *Phys. Rev. Research* **2**, 022047 (2020).
- [19] Ciarán Hickey, Christoph Berke, Panagiotis Peter Stavropoulos, Hae-Young Kee, and Simon Trebst, “Field-driven gapless spin liquid in the spin-1 kitaev honeycomb model,” *Phys. Rev. Research* **2**, 023361 (2020).
- [20] Iliia Khait, P. Peter Stavropoulos, Hae-Young Kee, and Yong Baek Kim, “Characterizing spin-one kitaev quantum spin liquids,” *Phys. Rev. Research* **3**, 013160 (2021).
- [21] Yu-Hsueh Chen, Jozef Genzor, Yong Baek Kim, and Ying-Jer Kao, “Excitation spectrum of spin-1 kitaev spin liquids,” *Phys. Rev. B* **105**, L060403 (2022).
- [22] P. Peter Stavropoulos, D. Pereira, and Hae-Young Kee, “Microscopic mechanism for a higher-spin kitaev model,” *Phys. Rev. Lett.* **123**, 037203 (2019).
- [23] Inhee Lee, Franz G. Utermohlen, Daniel Weber, Kyusung Hwang, Chi Zhang, Johan van Tol, Joshua E. Goldberger, Nandini Trivedi, and P. Chris Hammel, “Fundamental spin interactions underlying the magnetic anisotropy in the kitaev ferromagnet  $\text{CrI}_3$ ,” *Phys. Rev. Lett.* **124**, 017201 (2020).
- [24] Lebing Chen, Jae-Ho Chung, Bin Gao, Tong Chen, Matthew B. Stone, Alexander I. Kolesnikov, Qingzhen Huang, and Pengcheng Dai, “Topological spin excitations in honeycomb ferromagnet  $\text{CrI}_3$ ,” *Phys. Rev. X* **8**, 041028 (2018).
- [25] Lebing Chen, Jae-Ho Chung, Tong Chen, Chunruo Duan, Astrid Schneidewind, Igor Radelytskyi, David J. Voneshen, Russell A. Ewings, Matthew B. Stone, Alexander I. Kolesnikov, Barry Winn, Songxue Chi, R. A. Mole, D. H. Yu, Bin Gao, and Pengcheng Dai, “Magnetic anisotropy in ferromagnetic  $\text{CrI}_3$ ,” *Phys. Rev. B* **101**, 134418 (2020).
- [26] J.G. Rau and H.-Y. Kee, “Trigonal distortion in the honeycomb iridates: Proximity of zigzag and spiral phases in  $\text{Na}_2\text{IrO}_3$ ,” (2014), [arXiv:1408.4811](https://arxiv.org/abs/1408.4811).
- [27] Shigeki Onoda, “Effective quantum pseudospin-1/2 model for yb pyrochlore oxides,” *Journal of Physics: Conference Series* **320**, 012065 (2011).

- [28] Kate A. Ross, Lucile Savary, Bruce D. Gaulin, and Leon Balents, “Quantum Excitations in Quantum Spin Ice,” *Physical Review X* **1**, 1–10 (2011), [arXiv:1107.0761](#).
- [29] Jiří Chaloupka and Giniyat Khaliullin, “Hidden symmetries of the extended kitaev-heisenberg model: Implications for the honeycomb-lattice iridates  $A_2\text{IrO}_3$ ,” *Phys. Rev. B* **92**, 024413 (2015).
- [30] Jiefu Cen and Hae-Young Kee, “Strategy to extract kitaev interaction using symmetry in honeycomb mott insulators,” *Communications Physics* **2022** 5:1 **5**, 1–8 (2022).
- [31] P. Peter Stavropoulos, Xiaoyu Liu, and Hae-Young Kee, “Magnetic anisotropy in spin-3/2 with heavy ligand in honeycomb mott insulators: Application to  $\text{CrI}_3$ ,” *Phys. Rev. Research* **3**, 013216 (2021).
- [32] Stephen M. Winter, Ying Li, Harald O. Jeschke, and Roser Valentí, “Challenges in design of Kitaev materials: Magnetic interactions from competing energy scales,” *Phys. Rev. B* **93**, 214431 (2016).
- [33] Stephen M. Winter, Alexander A. Tsirlin, Maria Daghofer, Jeroen van den Brink, Yogesh Singh, Philipp Gegenwart, and Roser Valentí, “Models and materials for generalized Kitaev magnetism,” *Journal of Physics: Condensed Matter* **29**, 493002 (2017).
- [34] Lukas Janssen and Matthias Vojta, “Heisenberg-kitaev physics in magnetic fields,” *Journal of Physics: Condensed Matter* **31**, 423002 (2019).
- [35] Bevin Huang, Genevieve Clark, Efrén Navarro-Moratalla, Dahlia R. Klein, Ran Cheng, Kyle L. Seyler, Ding Zhong, Emma Schmidgall, Michael A. McGuire, David H. Cobden, Wang Yao, Di Xiao, Pablo Jarillo-Herrero, and Xiaodong Xu, “Layer-dependent ferromagnetism in a van der waals crystal down to the monolayer limit,” *Nature* **546**, 270–273 (2017).
- [36] Alexander Weiße and Holger Fehske, “Exact diagonalization techniques,” in *Computational Many-Particle Physics*, edited by H. Fehske, R. Schneider, and A. Weiße (Springer Berlin Heidelberg, Berlin, Heidelberg, 2008) pp. 529–544.